J|A|C|S
ARTICLES
Published on Web 01/09/2007

Rotational Dynamics in a Crystalline Molecular Gyroscope by Variable-Temperature ^{13}C NMR, ^{2}H NMR, X-Ray Diffraction, and Force Field Calculations

Tinh-Alfredo V. Khuong, Hung Dang, Peter D. Jarowski, Emily F. Maverick, and Miguel A. Garcia-Garibay*

Contribution from the Department of Chemistry and Biochemistry, University of California, Los Angeles, 405 Hilgard Avenue, Los Angeles, California 90095-1569

Received June 22, 2006; E-mail: mgg@chem.ucla.edu

Abstract: A combination of solid-state ^{13}C CPMAS NMR, ^{2}H NMR, X-ray-determined anisotropic displacement parameters (ADPs), and molecular mechanics calculations were used to analyze the rotational dynamics of 1,4-bis[3,3,3-tris(*m*-methoxyphenyl)propynyl]benzene (**3A**), a structure that emulates a gyroscope with a *p*-phenylene group acting as a rotator and two *m*-methoxy-substituted trityl groups acting as a stator. The line shape analysis of VT ^{13}C CPMAS and broad-band ^{2}H NMR data were in remarkable agreement with each other, with rotational barriers of 11.3 and 11.5 kcal/mol, respectively. The barriers obtained by analysis of ADPs obtained by single-crystal X-ray diffraction at 100 and 200 K, assuming a sinusoidal potential, were 10.3 and 10.1 kcal, respectively. A similar analysis of an X-ray structure solved from data acquired at 300 K suggested a barrier of only 8.0 kcal/mol. Finally, a rotational potential calculated with a finite cluster model using molecular mechanics revealed a symmetric but nonsinusoidal potential that accounts relatively well for the X-ray-derived values and the NMR experimental results. It is speculated that the discrepancy between the barriers derived from low and high-temperature X-ray data may be due to an increase in anharmonicity, or to disorder, at the higher temperature values.

Introduction

The past few years have witnessed a great deal of interest in the field of artificial molecular machines, both as isolated molecular units in solution[1,2] and when attached to various types of surfaces.[3,4] We[5,6] and others[7] have pursued the design and synthesis of molecules capable of forming crystalline arrays of highly dynamic and externally addressable molecular units. The information content of the desired structures should include features that facilitate certain conformational motions in the solid state in packing structures with parallel molecular alignment. Crystalline arrays of such units with reorienting electric and magnetic dipoles are expected to have interesting electrooptic and magnetooptic properties.[8,9] To test structural concepts and establish suitable methods to determine molecular dynamics in crystalline solids, we have recently pursued the design of *molecular gyroscopes* consisting of a phenylene *rotator* linked to shielding triarylmethyl or triptycyl[10,11] *stators* by a nearly barrierless dialkyne *axle*[12,13] (Figure 1). We have shown that crystals built with these structures possess a low packing density

(1) (a) Fletcher, S. P.; Dumur, F.; Pollard, M. M.; Feringa, B. L. *Science* **2005**, *310*, 80−82. (b) Balzani, V.; Credi, A.; Venturi, M. *Molecular Devices and Machines—A Journey into the Nano World*; Wiley-VCH: Weinheim, Germany, 2003. (b) Sauvage, J.-P. *Molecular Machines and Motors*; Springer-Verlag: New York, 2001; Vol. 99. (c) Kelly, T. R.; De Silva, H.; Silva, R. A. *Nature (London)* **1999**, *401* (6749), 150−152. (d) Leigh, D. A.; Wong, J. K. Y.; Dehez, F.; Zerbetto, F. *Nature (London)* **2003**, *424*, 174−179.

(2) (a) Siegel, J. *Science* **2005**, *5745*, 63−64. (b) Phillips, R.; Quake, S. R. *Phys. Today* **2006**, *59*, 38−43.

(3) (a) van Delden, R. A.; ter Wiel, M. K. J.; Pollard, M. M.; Vicario, J.; Koumura, N.; Feringa, B. L. *Nature* **2005**, *437*, 1337−1340. (b) Steuerman, D. W.; Tseng, H.-R.; Peters, A. J.; Flood, A. H.; Jeppesen, J. O.; Nielsen, K. A.; Stoddart, J. F.; Heath, J. R. *Angew. Chem., Int. Ed.* **2004**, *43*, 6486−6491. (c) Hernandez, R.; Tseng, H.-R.; Wong, J. W.; Stoddart, J. F.; Zink, J. I. *J. Am. Chem. Soc.* **2004**, *128*, 3370−3371. (c) Luo, Y.; Collier, C. P.; Jeppesen, J. O.; Nielsen, K. A.; DeIonno, E.; Ho, G.; Perkins, J. Tseng, H.-R. Yamamoto, T.; Stoddart, J. F. Heath, J. R. *ChemPhysChem* **2002**, *3*, 519.

(4) (a) Shirai, Y.; Osgood, A. J.; Zhao, Y.; Kell, K. F.; Tour, J. M. *Nano Lett.* **2005**, *5*, 2330−2334. (b) Shirai, Y.; Morin, J.-F.; Sasaki, T.; Guerrero, J. M.; Tour, J. M. *Chem. Soc. Rev.*, in press; published on the Web Aug 23, 2006.

(5) (a) Garcia-Garibay, M. A. *Proc. Natl. Acad. Sci. U.S.A.* **2005**, *102*, 10771−10776. (b) Karlen, S. D.; Garcia-Garibay, M. A. *Top. Curr. Chem.* **2006**, *262*, 179−227.

(6) (a) Dominguez, Z.; Dang, H.; Strouse, M. J.; Garcia-Garibay, M. A. *J. Am. Chem. Soc.* **2002**, *124*, 2398−2399. (b) Dominguez, Z.; Dang, H.; Strouse, M. J.; Garcia-Garibay, M. A. *J. Am. Chem. Soc.* **2002**, *124*, 7719−7727. (c) Dominguez, Z.; Khuong, T.-A. V.; Dang, H.; Sanrame, C. N.; Nunez, J. E.; Garcia-Garibay, M. A. *J. Am. Chem. Soc.* **2003**, *125*, 8827−8837.

(7) (a) Morimoto, M.; Irie, M. *Chem. Commun.* **2005**, 3895−3905. (b) Irie, M. In *Molecular Switches*; Feringa, B. L., Ed.; Wiley-VCH Verlag GmbH: Weinheim, Germany, 2001; pp 37−62. (c) Akutagawa, T.; Shitagami, K.; Nishihara, S.; Takeda, S.; Hasegawa, T.; Nakamura, T.; Hosokoshi, Y.; Inoue, K.; Ikeuchi, S.; Miyazaki, Y.; Saito, K. *J. Am. Chem. Soc.* **2005**, *127*, 4397−4402.

(8) (a) Liu, C.-Y.; Bard, A. J. *Acc. Chem. Res.* **1999**, *32*, 235−245. (b) Iverson, I. K.; Tam-Chang, S.-W. *J. Am. Chem. Soc.* **1999**, *121*, 5801−5802. (c) Wang, S. J.; Oldham, W. J.; Hudack, R. A.; Bazan, G. C. *J. Am. Chem. Soc.* **2000**, *122*, 5695−5709. (d) Salech, B. E. A.; Teich, M. C. *Fundamentals of Photonics*; Wiley-Interscience: New York, 1991. (e) Laurin, T. C. *The Photonics Dictionary*, 45th ed.; Lauring Publishing Co.: Pittsfield, MA, 1999; p D-107.

(9) (a) Adams, D. J.; McDonald, I. R. *Mol. Phys.* **1976**, *32*, 931. (b) Papazyan, A.; Maroncelli, M. *J. Chem. Phys.* **1991**, *95*, 9219−9241. (c) Collings, P. J.; Hird, M. *Introduction to Liquid Crystals*; Taylor and Francis, Ltd.: London, 1997. (d) Blinov, L. M. *Electro-Optic and Magneto-Optical Properties of Liquid Crystals*; Wiley: New York, 1983. (e) Guymon, G. A.; Dougan, L. A.; Martens, P. J.; Clarck, N. A.; Walba, D. M.; Bowman, C. N. *Chem. Mater.* **1998**, *10*, 2378−2388. (d) Walba, D. M.; Dyer, D. J.; Sierra, T.; Cobben, P. L.; Shao, R.; Clark, N. A. *J. Am. Chem. Soc.* **1996**, *118*, 1211−1212.

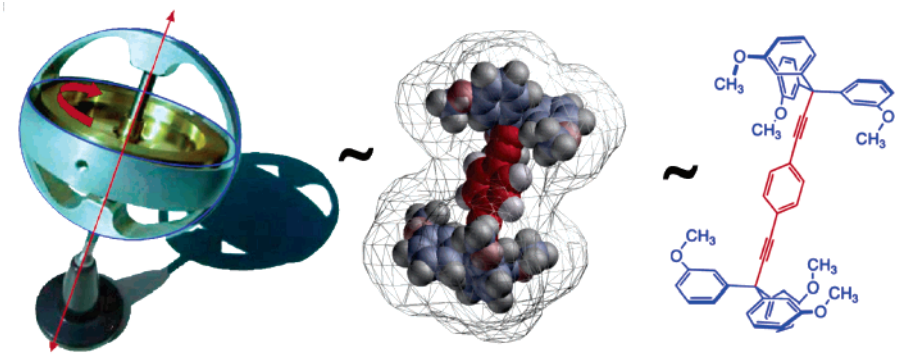

Figure 1. (Left) A simple gyroscope is an assembly consisting of a rotor with an axis of rotation that passes through its center of mass held together by an encapsulating frame. (Center) A space-filling model with a 4 Å solvent-accessible surface of a molecular gyroscope based on a phenylene rotor with a dialkyne axis (in red) and sterically encapsulating trityl groups (in blue). (Right) A line formula of the hexa-*m*-methoxytrityl derivative **3** studied in this paper.

Scheme 1

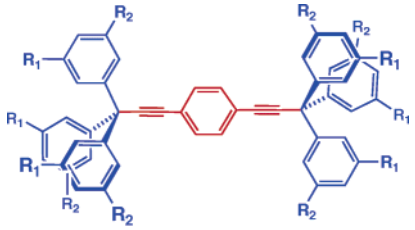

1: $R_1 = R_2 = H$
2: $R_1 = R_2 = tBu$
3: $R_1 = H$; $R_2 = OMe$
4: $R_1 = H$; $R_2 = O(CH_2)_8O$-

region around the "waist" of the molecule that facilitates the rotation of the central phenylene. It should be noted that molecular gyroscopes with rotational barriers that are higher than the available thermal energy (kT) are expected to undergo random back and forth displacements between energy minima (site exchange) in steps that depend on the symmetry of their rotational axes.[14] In contrast, molecular gyroscopes with barriers that are lower than the thermal energy may be expected to approach the dynamics of inertial rotators, such as that observed in the macroscopic objects.

Previous studies with crystals of the simple trityl derivative **1** ($R_1 = R_2 = H$, Scheme 1) using variable-temperature (VT) solid-state ^{13}C CPMAS and quadrupolar echo ^2H NMR experiments revealed a fast, 2-fold flipping motion, with a two-site exchange rate of 1.6 MHz at ca. 65 °C.[6] While remarkably fast for a phenylene group in a crystalline solid, this motion is much slower than that expected for an inertial rotator (ca. 10^{12} s^{-1}), and it may be best described as a stochastic process. It was shown that partial interdigitation of adjacent molecules in the lattice leads to steric barriers in the range of 12−14 kcal/mol for crystal forms with and without included benzene.[6] We subsequently showed that 3,5-di-*tert*-butyl substitution in each of the six trityl groups of compound **2** (Scheme 1, $R_1 = R_2 =$ tBu) allows for phenylene flipping with a rate $>10^8$ s^{-1} at 300 K.[15] Recently, along the way to prepare materials with the triply bridged compound **4** ($R_1 = H$, $R_2 = -O(CH_2)_{10}O-$), which more closely emulates the structure of macroscopic gyroscopes, we synthesized and characterized the hexa-*m*-methoxy-substituted molecular gyroscope **3** (Scheme 1, $R_1 = H$, $R_2 = OMe$).[16] The structure of **3** was particularly interesting because of its large stereochemical diversity, which arises from a remarkably rich conformational landscape.[17] With the help of single-crystal X-ray diffraction, differential scanning calorimetry (DSC), polarized microscopy, and solid-state ^{13}C CPMAS NMR,[18] we documented up to seven distinct phases and six phase transitions. We showed that a benzene-containing clathrate (form **A**) desolvates at 140 °C in a first-order phase transition to form a solvent-free crystal phase identical to that obtained when crystals are grown from $CHCl_3$ (form **B**). Three additional solvent-free phases (forms **C**−**E**) were documented at higher temperatures, before melting to a stable liquid phase occurred at 181 °C, and two more by crystallization at lower temperatures.[16] A close inspection of the ^{13}C CPMAS NMR spectrum of the benzene-containing phase suggested a dynamic process consistent with the desired rotary motion. In this paper, we report a detailed analysis of this process by VT ^{13}C CPMAS NMR between 245 and 281 K, quadrupolar echo ^2H NMR in the range of 245−367 K, and analysis of anisotropic displacement parameters (ADPs) of single-crystal X-ray diffraction data acquired at 100, 200, and 300 K. While remarkably consistent activation energies

(10) (a) Godinez, C. E.; Zepeda, G.; Garcia-Garibay, M. A., *J. Am. Chem. Soc.* **2002**, *124*, 4701−4707. (b) Godinez, C. E.; Zepeda, G.; Garcia-Garibay, M. A. *J. Am. Chem. Soc.* **2002**, *124*, 4701−4707.

(11) For molecular gyroscopes based on transition-metal complexes please see: (a) Wang, L.; Hampel, F.; Gladysz, J. A. *Angew. Chem., Int. Ed.* **2006**, *45*, 4372−4375. (b) Narwara, A. J.; Shima, T.; Hampel, F.; Gladysz, J. A. *J. Am. Chem. Soc.* **2006**, *128*, 4962−4963. (c) Shima, T.; Hampel, F.; Gladysz, J. A. *Angew. Chem., Int. Ed.* **2004**, *43*, 5537−5540.

(12) The terminology used here to describe the components of an artificial molecular rotor was recently suggested by Kottas et al.: Kottas, G. S.; Clarke, L. I.; Horinek, D.; Michl, J. *Chem. Rev.* **2005**, *105*, 1281−1376.

(13) (a) Saebo, S.; Almolof, J.; Boggs, J. E.; Stark, J. G. *J. Mol. Struct.: THEOCHEM* **1989**, *200*, 361−373. (b) Abramenkov, A. V.; Almenningen, A.; Cyvin, B. N.; Cyvin, S. J.; Jonvik, T.; Khaikin, L. S.; Rommingin, C.; Vilkov, L. V. *Acta Chem. Scand.* **1988**, *A42*, 674−678. (c) Sipachev, V. A.; Khaikin, L. S.; Grikina, O. E.; Nikitin, V. S.; Traettberg, M. *J. Mol. Struct.* **2000**, *523*, 1−22. (d) Seminario, J.; Zacarias, A. G.; Tour, J. M. *J. Am. Chem. Soc.* **2000**, *122*, 3015−3020. (e) Miteva, T.; Palmer, L.; Kloppenburg, L.; Neher, D.; Bunz, U. H. F. *Macromolecules* **2000**, *33*, 652−654.

(14) Karlen, S. D.; Ortiz, R.; Chapman, O. L.; Garcia-Garibay, M. A. *J. Am. Chem. Soc.* **2005**, *127*, 6554−6555.

(15) Khuong, T.-A.; V.; Zepeda, L. G.; Ruiz, R.; Khan, S. I.; Garcia-Garibay, M. A. *Cryst. Growth Des.* **2004**, *4*, 15−18.

(16) Nuñez, J. E.; Khuong, T.-A. V.; Campos, L. M.; Farfán, N.; Dang, H.; Karlen, S. D.; Garcia-Garibay, M. A. *Cryst. Growth Des.* **2006**, *6*, 866−873.

(17) Eliel, E. L.; Wilen, S. H. *Stereochemistry of Organic Compounds*; John Wiley & Sons: New York, 1994.

(18) Pines, A.; Gibby, M. G.; Waugh, J. S. *J. Chem. Phys.* **1973**, *59*, 569−590. For reviews and examples of the CPMAS experiment please see: (a) Schaefer, J.; Stejskal, E. O. *Top. Carbon-13 NMR Spectrosc.* **1979**, *3*, 283−324. (b) Fyfe, C. A. *Solid State NMR for Chemists*; CFC Press: Guelph, Ontario, 1983. (c) Yannoni, C. S. *Acc. Chem. Res.* **1982**, *15*, 201−208. (d) Lyerla, J. R.; Yannoni, C. S.; Fyfe, C. A. *Acc. Chem. Res.* **1982**, *15*, 208−216. (e) Harris, K. D. M.; Aliev, A. E. *Chem. Br.* **1995**, *31*, 132−136. (f) Kitchin, S. J.; Xu, M.; Serrano-Gonzalez, H.; Coates, L. J.; Zaka, Ahmed, S.; Glidewell, C.; Harris, K. D. *J. Solid State Chem.* **2006**, *179*, 1335−1338.

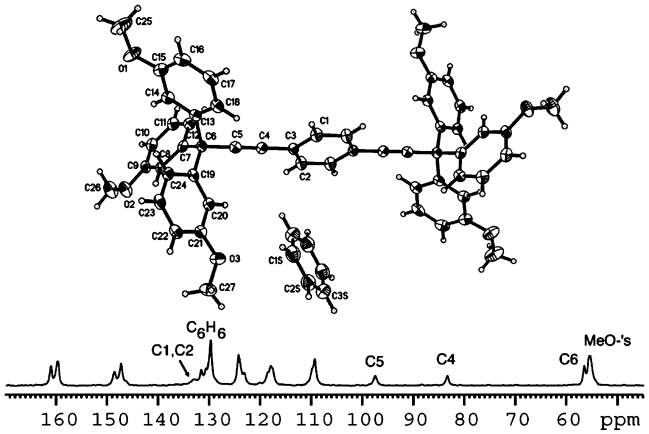

Figure 2. ORTEP structure with atom numbering, and partially assigned ^{13}C CPMAS NMR spectrum of **3A** acquired at 300 K.

of 11.7 and 11.5 kcal/mol were estimated by the two NMR methods, ADP analysis with a simple sinusoidal potential suggested barriers of 10.3, 10.1, and 8.0 kcal/mol at 100, 200, and 300 K, respectively.

Results and Discussion

The synthesis of compound **3** by Pd(0)-catalyzed coupling of the (hexa-*m*-methoxytrityl)acetylene and 1,4-diiodobenzene was reported in a previous paper.[16] Phenylene deuterated samples for ^{2}H NMR studies were prepared in the same manner using commercial 1,4-dibromobenzene-d_4. As expected for the small size of the methoxy substituents, the solution ^{1}H and ^{13}C NMR spectra revealed a time-averaged symmetric structure, with local 3-fold and 2-fold symmetries for the triarylmethyl and phenylene groups. Although the relatively high thermal stability of the benzene clathrate **3A** near ambient temperature had been previously documented, all the experiments reported in this paper were carried out with samples that had been freshly crystallized from benzene.

Rotational Dynamics of Clathrate 3A by Coalescence Analysis of ^{13}C CPMAS Solid-State NMR Spectra. While running ^{13}C CPMAS NMR spectra of the solvent clathrate **3A** as a function of temperature, we noticed that relatively small variations in temperature resulted in significant changes in the line width of a signal at ca. 132 ppm. The molecular structure of **3A** is illustrated in Figure 2 along with a ^{13}C CPMAS NMR spectrum acquired at 300 K. Molecular gyroscope **3A** possesses a center of inversion in the central phenylene, giving rise to 27 (rather than 54) crystallographically and magnetically nonequivalent carbons. With inductive, resonance, and field effects, the spectrum presents relatively good chemical shift dispersion among the various types of carbons. Signals at 55.0 and 56.5 ppm correspond to the three crystallographically nonequivalent methoxy groups and the quaternary carbon signal (C6), respectively. The two alkyne signals resonate at 83 (C4) and 97 (C5) ppm. The aromatic carbons attached to the methoxy groups and the nonprotonated aromatic *ipso* carbons appear as two signals each, at 160 and 147 ppm, respectively. Carbon atoms *ortho* and *para* to the methoxy substituents resonate in groups at ca. 109, 117, and 123 ppm. The latter signal overlaps with a nonprotonated phenylene carbon (C3), which occurs at 122 ppm. Finally, the remaining trityl signals occur at ca. 130 ppm, where they overlap with the protonated phenylene signals C1 and C2 that undergo exchange as a function of temperature.

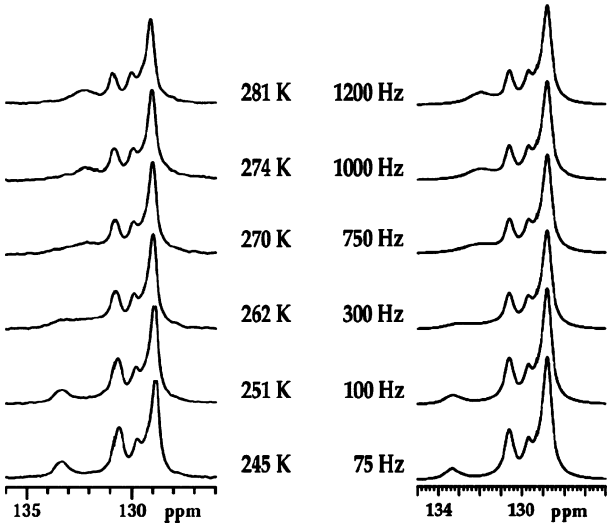

Figure 3. Simulated (right) and experimental (left) ^{13}C CPMAS NMR spectra of crystals of **3A**. The temperature of the experiment and the rates of exchange used in the line shape simulations are indicated next to the corresponding spectra.

A close analysis of the region corresponding to C1 and C2 for spectra acquired between 245 and 183 K is illustrated in Figure 3 along with line shape simulations carried out with the program gNMR.[19] Signals corresponding to carbon atoms in the benzene molecule and *meta* to the methoxy group, like the rest of the spectrum, remain unchanged within this temperature range. However, clear variations as a function of increasing temperature can be observed for signals that start at ca. 133.4 and 130.6 ppm at 245 K, although the latter overlaps with a signal from the trityl carbons. The experimental data were simulated by inputting the aforementioned chemical shifts at the slow exchange limit assuming a Gaussian line shape with a heterogeneous broadening of 35 Hz. When the rate of exchange was varied as a function of temperature, an excellent matching of the experimental spectra was observed.[20] With exchange rates varying from 75 s^{-1} at 245 K to 1200 s^{-1} at 281 K, we constructed an Arrhenius plot to determine a barrier of 11.7 kcal/mol and a preexponential factor of 1.7×10^{12} s^{-1}. These values are similar to those previously determined for unsubstituted **1**, where the flipping motion of the phenylene group in the solvent clathrate documented by VT ^{13}C CPMAS NMR has a barrier of 12.8 kcal/mol.[6] The magnitude of the preexponential factor is in good agreement with a rotational frequency of 2.4×10^{12} s^{-1} calculated for a phenylene free rotor from its moment of inertia along the 1,4-axis.[21]

Rotational Dynamics of Clathrate 3A by Quadrupolar Echo ^{2}H NMR. To confirm the results from the ^{13}C CPMAS coalescence experiment, we decided to investigate the rate of phenylene rotation by quadrupolar echo ^{2}H NMR. It has been well established that solid-state ^{2}H NMR is one of the most powerful methods to determine internal molecular dynamics in the solid state.[22] As deuterium NMR is largely dominated by

(19) *gNMR*, version 5.0; Adept Scientific, Inc.: Bethesda, MD, 2003.
(20) Small adjustments to the signal intensities were used in the simulations to compensate for changes assigned to varying cross-polarization and rotating frame relaxation rates as a function of temperature.
(21) The principal moment of inertia along the phenylene 1,4-axis is ca. 80.1 g/(mol Å^2). The rotational frequency for a free rotor was calculated as described by Kawski: Kawski, A. *Crit. Rev. Anal. Chem.* **1993**, *23*, 459−529.
(22) Hoatson, G. L.; Vold, R. L. *NMR Basic Princ. Prog.* **1994**, *32*, 1−67.

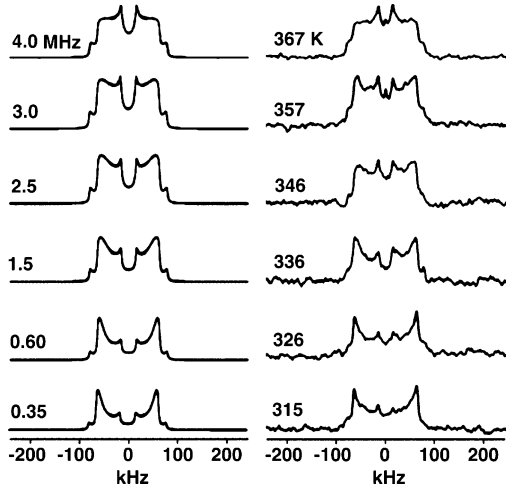

Figure 4. Representative examples of simulated (left) and experimental (right) solid-state ^{2}H NMR spectra for benzene clathrate **3A**.

the orientation-dependent interaction between the nuclear spin and electric quadrupole moment at the nucleus, the characteristically broad spectrum from molecules in static powdered samples is strongly affected by internal molecular motions in the solid state. The signal of any static ^{2}H spin would consist of a doublet with a quadrupolar splitting, $\Delta\nu$, that depends on the orientation angle β that the C$-^2$H bond makes with respect to the external field:

$$\Delta\nu = (3/4)(e^2q_{zz}Q_m/h)(3\cos^2\beta - 1) = (3/4)(\mathrm{QCC})(3\cos^2\beta - 1)$$

Q_m represents the electric quadrupole moment of the deuteron, e and h are the electron charge and Planck constant, and q_{zz} is the magnitude of the principal component of the electric field gradient tensor, which lies along the C$-^2$H bond. Since powdered samples have molecules with all values of β represented, a collection of doublets gives rise to a broad symmetric spectrum with two maxima and two shoulders known as a Pake or powder pattern. Changes in the spectra occur when the C$-^2$H bonds experience reorientations that reduce the range of their magnetic interactions by dynamic averaging, with the dynamics of aromatic deuterons being among the best characterized.[23] Since the slow exchange limit of ^{2}H NMR is ca. 10^4 s^{-1}, measurements in the case of **3A** had to be carried out at temperatures that are significantly higher than those accessible by the ^{13}C CPMAS coalescence method. However, to avoid complications from solvent efflorescence and a phase transition, we restricted our analysis to finely powdered samples freshly crystallized from benzene with spectral acquisitions within a temperature range between 300 and 377 K, which is well below the desolvation phase transition temperature of 413 K.

As illustrated in Figure 4, spectra were simulated with a program described by Nishikiori et al.[24] using a model that assumes a 2-fold (180°) phenylene flip,[25] a quadrupolar coupling constant of 180 kHz, and exchange rates between 10 kHz and 10 MHz. Arrhenius analysis of the data provided a rotational barrier of 11.6 ± 2.0 kcal/mol and a preexponential factor of (3.5 ± 3.0) × 10^{13} s^{-1}.[26] While there is a large uncertainty in these values, the calculated barrier is consistent with that determined from the coalescence data. The larger discrepancy in the preexponential factor may be ascribed to the different temperature regimes of the two experiments and to the temperature dependence of the activation free energy (entropic factors), which is not accounted for by the Arrhenius equation.

Rotational Dynamics of Clathrate 3A by X-Ray Atomic ADP Analysis. Shortly after the discovery of X-ray diffraction in 1913, Debye[27] showed that increasing the temperature reduces the diffraction intensities, especially at large scattering angles, by increasing the extent of vibration of atoms about their average positions. Cruickshank reported later that anisotropic "vibration parameters" for aromatic systems could be interpreted in terms of molecular rigid-body motion[28] and thus be related to the spectroscopic and thermodynamic properties[29] of crystals. Since the pioneering work by Cruickshank, many crystallographers have made remarkable contributions toward the understanding of crystallographic ADPs and their utility in understanding molecular motions in crystals. In more recent years, Dunitz,[30,31] Schomaker,[30] Maverick,[31,32] Trueblood,[30−32] and Bürgi[33] have influenced the way chemists use crystallographic ADPs. Given the dynamic information determined from ^{13}C CPMAS coalescence and ^{2}H NMR quadrupolar line shape analysis, we decided to explore the use of X-ray-derived ADPs to investigate the nature of the rotational potential in benzene clathrate **3A**.

Single-crystal diffraction data for the benzene clathrate **3A** were acquired at 100, 200, and 300 K using the same crystal specimen.[34] The ADPs from the three data sets are illustrated by ORTEP diagrams drawn at the 30% probability level with a view down the plane of the central phenylene ring in Figure 5. The size and direction of the elongated ellipsoid axes of the central phenylene carbons (C1 and C2 and their symmetry-

(23) (a) Cholli, A. L.; Dumais, J. J.; Engel, A. K.; Jelinski, L. W. *Macromolecules* **1984**, *17*, 2399−2404. (b) Rice, D. M.; Witebort, R. J.; Griffin, R. G.; Meirovich, E.; Stimson, E. R.; Meinwald, Y. C.; Freed, J. H.; Scheraga, H. A. *J. Am. Chem. Soc.* **1981**, *103*, 7707. (c) Rice, D. M.; Meinwald, Y. C.; Scheraga, H. A.; Griffin, R. G. *J. Am. Chem. Soc.* **1987**, *109*, 1636−1640. (d) Rice, D. M.; Blume, A.; Herzfeld, J.; Wittebort, R. J.; Huang, T. H.; DasGupta, S. K.; Griffin, R. G. *Biomol. Stereodyn., Proc. Symp.* **1981**, *2*, 255−270.

(24) Nishikiori, S.; Soma, T.; Iwamoto, T. *J. Inclusion Phenom.* **1997**, *27*, 233−243.

(25) (a) Wehrle, M.; Hellmann, G. P.; Spiess, H. W. *Colloid Polym. Sci.* **1987**, *265*, 815−822. (b) Spiess, H. W. *Colloid Polym. Sci.* **1983**, *251*, 193−209. (c) Reichert, D.; Hempel, G.; Zimmermann, H.; Schneider, H.; Luz, Z. *Solid State Nucl. Magn. Reson.* **2000**, *18*, 17−36.

(26) The uncertainity in the activation parameters was estimated from simulations with the highest and lowest exchange rates that reasonably matched the experimental spectra at each temperature value.

(27) Debye, P. *Verh. Dtsch. Phys. Ges.* **1913**, *15*, 738−752.

(28) Cruickshank, D. W. J. *Acta Crystallogr.* **1956**, *9*, 754−756.

(29) Cruickshank, D. W. J. *Acta Crystallogr.* **1956**, *9*, 1005−1011.

(30) (a) Dunitz, J. D.; Schomaker, V.; Trueblood, K. N. *J. Phys. Chem.* **1988**, *92*, 856−867. (b) Schomaker, V.; Trueblood, K. N. *Acta Crystallogr.* **1998**, *B54*, 507−514.

(31) Dunitz, J. D.; Maverick, E. F.; Trueblood, K. N. *Angew. Chem., Int. Ed. Engl.* **1988**, *27*, 880−895.

(32) Maverick, E. F.; Knobler, C. B.; Khan, S. I.; Canary, J. W.; Dicker, I. B.; Trueblood, K. N. *Helv. Chim. Acta* **2003**, *86*, 1309−1319.

(33) Bürgi, H.-B.; Capelli, S. C. *Helv. Chim. Acta* **2003**, *86*, 1625−1640.

(34) Structure at 100 K: a = 6.9849(10) Å, b = 10.1656(15) Å, c = 17.697(3) Å, α = 77.320(2)°, β = 82.054(2)°, γ = 73.833(2)°, V = 1173.4(3) Å^3, $P\bar{1}$, Z = 1, formula $C_{54}H_{46}O_6{\cdot}C_6H_6$, R1 = 0.0611 (2911 reflections), wR2 = 0.1753 (5423 reflections), 301 parameters, Mo Kα, θ_{full} = 26.0°, GOF = 0.962. Structure at 200 K: a = 7.0590(12) Å, b = 10.1724(17) Å, c = 17.820(3) Å, α = 77.152(3)°, β = 81.507(3)°, γ = 73.412(3)°, V = 1190.8-(3) Å^3, R1 = 0.0657 (2415 reflections), wR2 = 0.1871 (5472 reflections), 301 parameters, Mo Kα, θ_{full} = 26.0°, GOF = 0.939. Structure at 300 K: a = 7.116(4) Å, b = 10.145(5) Å, c = 17.823(9) Å, α = 77.253(9)°, β = 80.996(8)°, γ = 73.084(8)°, V = 1194.7(10) Å^3, R1 = 0.0656 (1392 reflections), wR2 = 0.1772 (5139 reflections), 301 parameters, Mo Kα, θ_{full} = 20.5°, GOF = 0.772. The much lower number of observed reflections, the low value of θ_{full}, and the low goodness-of-fit indicate a loss of long-range order in the crystal at 300 K. Refinement of a disorder model for the solvent benzene, and limiting θ_{max} to 23.0°, increases the GOF to 0.879 (R1 = 0.0681 (1363 reflections), wR2 = 0.1760 (3242 reflections), 278 parameters).

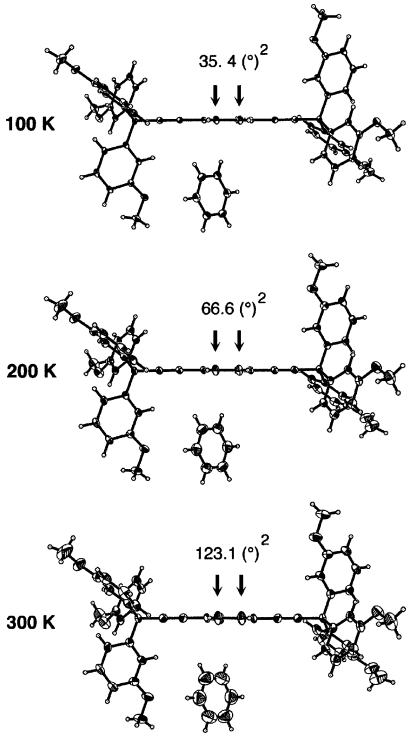

Figure 5. ORTEP diagrams of benzene clathrate **3A** from data taken at 100, 200, and 300 K, with ellipsoids drawn at the 30% probability level. Values for $\langle\varphi^2\rangle$, the mean-square libration amplitude of the phenylene group about the long molecular axis, are shown (please see the text).

related atoms) suggest that motion about the long molecular axis can occur even at 100 K. Although in-plane rotation of the benzene molecule and libration of the methoxy groups and trityl aromatic groups are also evident by the direction of elongation in their ellipsoids, we centered our attention on the phenylene group. As expected from an increase in thermal energy, the phenylene carbon ellipsoids (as well as all others in the structure) are more elongated as the temperature increases to 200 and 300 K.

To analyze the ADPs in terms of the rotational energy profile for the central phenylene, we used the Thermal Motion Analysis program (THMA14C) written by Schomaker and Trueblood,[30] which was subsequently adapted in WinGX by Farrugia.[35] A model accounting for translation, libration, and screw motion (TLS model) is obtained from the atomic displacement tensors with a least-squares procedure. One or more attached rigid groups (ARGs) may be added to model internal motion in an otherwise rigid molecule. After a mean-square torsional amplitude, $\langle\varphi^2\rangle$, was obtained for the phenylene fragment at each of the three temperatures, a quadratic force constant for the torsional motion was estimated to approximate a periodic cosine rotational potential, V, of the form $V = (V_2/2)[1 - \cos(2\phi)]$, where V_2 is the 2-fold rotational barrier.

In the case of **3A**, a rigid bond test,[36] based on the matrix of differences in mean-square displacement amplitudes (ΔMSDA, pm^2) between bonded atoms, shows that the molecule as a whole is not "rigid"; however, the eighteen-atom central frame, including the rotating phenylene group, the attached triple bond, the trityl carbon C6, and the three ipso C atoms anchoring the trityl aromatics (C1, C2, C3, C4, C5, C6, C7, C13, and C19 and their symmetry-related equivalents, Figure 2), satisfies the test fairly well.[37] Analysis of this framework with the phenylene C atoms C1, C2, C1′, and C2′ as an ARG rotating about the C4−C3 axis gives mean-square displacement amplitudes, $\langle\varphi^2\rangle$, of 35.5, 63.7, and 123.6 deg^2 and calculated barriers to torsional motion of 10.3, 10.6, and 8.0 kcal/mol at 100, 200, and 300 K, respectively. Motion of the frame as a whole is negligible. However, better agreement is obtained by analyzing internal torsional motion by the TLS method within an eight-carbon rigid frame that includes the rotating phenylene group and the attached alkyne carbons (C4, C1, C2, C3, C1′, C2′ C3′, and C4′, Figure 2). The rigid bond test and agreement factor values are lower, and the libration amplitudes about the C4−C4′ axis are essentially the same: 35.4, 66.6, and 123.1 deg^2 for motion at 100, 200, and 300 K, respectively (Figure 5). With these values, 2-fold rotational barriers of 10.3, 10.1, and 8.0 kcal/mol were calculated at 100, 200, and 300 K, respectively. The estimated uncertainty in the barrier height is about 2 kcal/mol. The decrease in the calculated rotational barrier at 300 K may be due to limitations from the model, which assumes a simple harmonic approximation to the torsional potential[31] and a partial loss of benzene molecules from the crystal lattice, or to further thermal or static disorder, as suggested by the low resolution of the data.[37]

Potential Energy Profile. It has been shown that molecular mechanics calculations can be a simple but valuable tool to evaluate the extent of nonbonding interactions for molecules undergoing displacements in crystalline systems as a result of topochemical reactions[38] and rotational trajectories in polar and nonpolar molecular compasses and gyroscopes.[39,40] In nonpolar systems, the rotational potential is almost exclusively dependent on the immediate steric environment so that changes in energy can be reasonably described by exploring the trajectory of a test molecule at the center of a relatively small molecular cluster. Using this simple method, agreement between the calculated and experimental values can be within a few kcalories per mole.[39]

(35) Farrugia, L. J. *J. Appl. Crystallogr.* **1999**, *32*, 837−838.
(36) Hirshfeld, F. L. *Acta Crystallogr.* **1976**, *A32*, 239−244.

(37) Thermal motion analysis: For the 18-carbon atom central framework, ⟨ΔMSDA⟩ values of 0.0039, 0.0040, and 0.0089 pm^2 for the three temperatures are to be compared with mean standard deviations of U_{obsd} of 0.0012, 0.0015, and 0.0026 pm^2, respectively, giving ⟨ΔMSDA⟩/⟨esd-(*U*)⟩ values of 3.2, 2.7, and 3.4. The maximum libration amplitude for the frame is 0.47, 0.79, and 0.44 deg^2, with $\langle\varphi^2\rangle$ for the phenylene ARG of 35.5(12.3), 63.7(15.2), and 123.6(26.9) deg^2, agreement factors $R = 0.157$, 0.126, and 0.158 (for all *U* values), and GOF = 2.38, 2.27, and 2.16 for data sets at 100, 200, and 300 K, respectively. These libration amplitudes give barrier heights of 10.3(2.8), 10.6(2.0), and 8.0(1.3) kcal/mol. For the eight-carbon central phenylene with C4 and C4′, ⟨ΔMSDA⟩ values are 0.0027, 0.0039, and 0.0095 pm^2 and ⟨esd(*U*)⟩ values are 0.0012, 0.0016, and 0.0029 pm^2 for 100, 200, and 300 K, respectively, giving ⟨ΔMSDA⟩/⟨esd(*U*)⟩ values of 2.2, 2.4, and 3.3. Libration amplitudes about the C4−C4′ axis are 35.4, 66.6, and 123.1 deg^2, with agreement factors $R = 0.106$, 0.069, and 0.114 (for all *U* values) and GOF = 2.06, 1.60, and 2.00 for data sets at the three temperatures. Refinement of the 300 K structure with a disordered benzene model and $\theta_{max} = 23.0°$ does not change the results appreciably for the phenylene rotor ($\langle\varphi^2\rangle$ = 125.1 (30.1) deg^2), but ⟨ΔMSDA⟩ and ⟨esd(*U*)⟩ values are higher, at 0.0087 and 0.0032 pm^2, respectively.
(38) (a) Keating, A. E.; Shin, S. H.; Houk, K. N.; Garcia-Garibay, M. A., *J. Am. Chem. Soc.* **1997**, *119*, 1474−1475. (b) Keating, A. E.; Shin, S. H.; Huang, F. K.; Garrell, R. L.; Garcia-Garibay, M. A. *Tetrahedron Lett.* **1999**, *40*, 261−264. (c) Garcia-Garibay, M. A.; Houk, K. N.; Keating, A. E.; Cheer, C. J.; Leibovitch, M.; Scheffer, J. R.; Wu, L.-C. *Org. Lett.* **1999**, *1*, 1279−1281. (d) Zimmerman, H. E.; Zhu, Z., *J. Am. Chem. Soc.* **1994**, *116*, 9757−9758.
(39) (a) Horansky, R. D.; Clarke, L. I.; Khuong, T.-A. V; Jarowski, P. D.; Garcia-Garibay, M. A.; Price, J. C. *Phys. Rev. B* **2005**, *72*, 014302. (b) Horansky, R. D.; Clarke, L. I.; Karlen, S. D.; Santillan, R.; Jarowski, P. D.; Garcia-Garibay, M. A.; Price, J. C. *Phys. Rev. B* **2006**, *74*, 054306.
(40) Jarowski, P. D.; Houk, K. N.; Garcia-Garibay, M. A. *J. Am. Chem. Soc.*, submitted for publication.

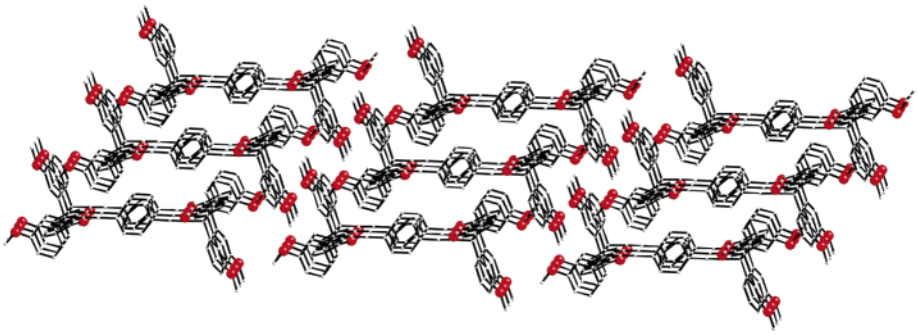

Figure 6. Cluster (3 × 3 × 3) of **3A** used to calculate the potential energy diagram for rotation of the central phenylene (hydrogen atoms removed for clarity).

To analyze the rotational profile of **3A**, we have selected the MM3 force field[41] and a model that includes a 3 × 3 × 3 array of molecular rotors (Figure 6) with atomic positions directly extracted from the crystal structure at 100 K. The model includes 18 benzene molecules, which are obscured by the rotator phenylene rings in the depiction above. The packing arrangement of **3A** can be described in terms of columns of alternating benzene molecules and rotator moieties, with the benzene molecules taking an edge-on orientation with respect to the phenylene rotators. The cluster structure is maintained by constraining the original positions of certain atoms, while allowing the relaxation of all others. A translational constraint is implemented by fixing the positions of all the trityl carbons to ensure that the relative position and orientation of the molecules will not change appreciably in the lattice. Whole body rotation about the long molecular axis is prevented by constraining the position of all the *ipso* carbons in the two trs(*m*-methoxyphenyl)methanes. Both of these constraints are applied to all molecular gyroscopes except for the central one and the two trityl groups that are in closest contact with the test rotator. By allowing full relaxation of the most proximal groups, we seek a more realistic representation of all the local geometric effects that may be taking place upon internal rotation. Thus, using this model, the dihedral angle of the central phenylene rotator is driven in steps of 10° over 360° and the structure minimized at each stage.[42] The resulting potential energy profile is shown in Figure 7.

As illustrated in Figure 7 (solid line), although the potential energy profile is a periodic function with equivalent minima every 180°, it is not a simple sine function. The rotational transition states do not occur at 90° and 270°, but are displaced closer to the origin by ca. 20°, occurring near 70° and 250°, respectively. The calculated rotational barrier of 12.9 kcal/mol is in reasonable agreement with the experimental estimates of 11.5 and 11.7 kcal/mol obtained by NMR and with the values of 10.3 and 10.1 kcal/mol obtained at low temperature by ADP analyses.

To test the possibility that the experimental barrier of 8.0 kcal/mol estimated from ADP analysis at 300 K may result from partial loss of benzene at this temperature, the rotational potential was also calculated for a model where the two benzene molecules in contact with the rotating phenylene are removed. The resulting rotational potential, shown with a dashed line in

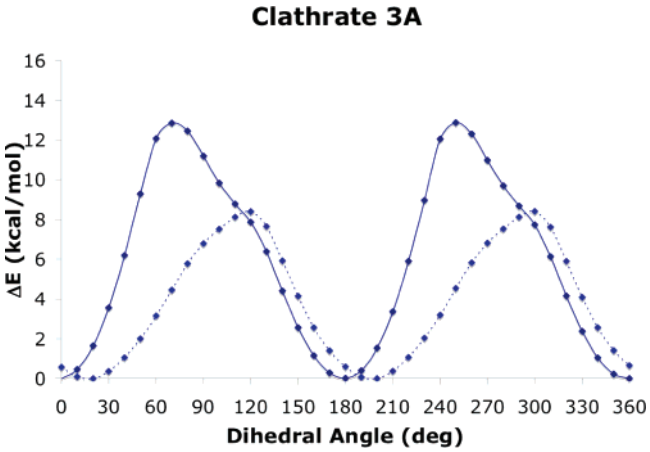

Figure 7. (Solid line) MM3 rotational potential energy profile of clathrate **3A** for the dihedral angle of the phenylene rotator driven in steps of 10° over 360° using the model in Figure 6. (Dashed line) Rotational potential when the two most proximal benzene molecules are removed (partially desolvated).

Figure 7, is also anharmonic, with maxima and minima that are offset from the solvated model. The barrier height of the partially desolvated structure is considerably reduced to a value of only 8.4 kcal/mol, which is in reasonable agreement with the X-ray estimation of 8.0 kcal/mol. The low resolution of the 300 K X-ray data may indeed be due, in part, to solvent loss or disorder.[34]

To model the region relevant to the libration amplitudes derived from the X-ray ADP analysis, we also calculated the potential energy profile near the equilibrium position by driving the dihedral angle of the rotator by ±20° in steps of 1° with atomic positions derived from the 300 K data. Notably, fitting these data to a sinusoidal function[43] gave a value of 10.9 kcal/mol for the barrier, which is very close to the values calculated at 100 and 200 K, suggesting that the equilibrium positions do not change significantly as a function of temperature. Given that the large librational displacement amplitudes at 300 K appear not to result from a lower barrier, it is likely that they may be the result of a greater anharmonicity in the free energy surface, perhaps related to coupled motions[40] and crystal lattice "softening" occurring at higher temperatures. As illustrated in Figure 8, this interpretation would imply that the free energy surface, on average, would have increasingly different curvatures near the minima and maxima as the temperature increases. These

(41) Allinger, N. L.; Yuh, Y. H.; Lii, J.-H. J. *Am. Chem. Soc.* **1989**, *111*, 8551.
(42) Mohamadi, F.; Richards, N.; Guida, W. C.; Liskamp, R.; Lipton, M; Caufield, D.; Chang, T.; Hendrickson, T.; Still, W. *J. Comput. Chem.* **1990**, *11*, 440.
(43) The data are fit using the Levenberg−Marquardt fitting algorithm. The χ^2 value for the fit is 0.17. *Pro Fit*, version 5.6.4, trial version; QuantumSoft: Uetikon am See, Switzerland; http://www.quansoft.com.

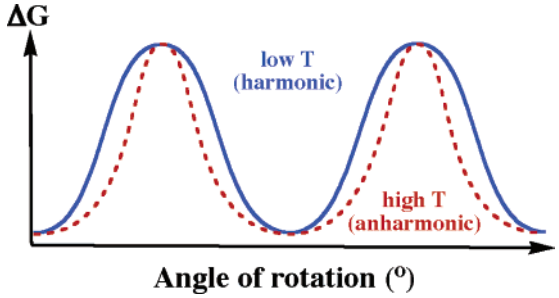

Figure 8. Hypothetical variations in the free energy surface for the rotation of the phenylene group in **3A**. An increase in anharmonicity at higher temperature would allow for the larger amplitude oscillations suggested by the ADP analysis, without significantly affecting the rotational barrier, as suggested by dynamic NMR.

variations would give rise to larger amplitude oscillations about the minimum but would not be observable in terms of large distortions in equilibrium positions and would not affect the height of the barrier.

Conclusions

A determination of the 2-fold flipping rotational dynamics of compound **3A** by three different experimental methods and computational analysis leads to remarkable agreement and valuable insights. The agreement observed between activation energies determined by ^{13}C CPMAS (11.7 kcal/mol) and ^{2}H NMR (11.5 kcal/mol) is remarkable. Similarly, the results obtained from analysis of the anisotropic displacement parameters from X-ray diffraction data acquired at 100 K (10.3 kcal/mol) and 200 K (10.1 kcal/mol) were equally consistent with each other and within 1 kcal/mol of the NMR results. A relatively simple molecular mechanics model used to determine the corresponding torsional potential resulted in a barrier of 12.9 kcal/mol, which is also very close to the NMR experimental values. These results also revealed a nonharmonic potential, which may explain the disagreement between the NMR and low-temperature X-ray results. The only experimental observation that was well outside the range came from ADP analysis of X-ray data acquired at 300 K, which suggested a barrier of only 8.0 kcal/mol, which, we believe, may reflect an increased anharmonicity in the free energy surface at the higher temperatures. It is interesting to note that rotational motion in crystalline solids can take place with frequencies and energy barriers of the same order of magnitude as those observed in a large number of molecular rotors in solution media.[12] Additional examples with higher symmetry rotators now in progress may help reveal whether the suggested anharmonicities may correlate with the magnitude of the angular displacement between degenerate minima.

Acknowledgment. This work was supported by the National Science Foundation through Grants DMR-0307028 and DMR-0605688. P.D.J. is grateful for the support of the American Chemical Society Organic Division Fellowship sponsored by Organic Reactions, Inc. We thank Steve Karlen for valuable discussions and help.

Supporting Information Available: Thermal motion analysis using anisotropic displacement parameters (PDF) and crystallographic information files (CIFs) for compound **3A** acquired at 100, 200, and 300 K and an additional CIF of the 300 K data for a model that considers benzene disorder. This material is available free of charge via the Internet at http://pubs.acs.org.

JA064325C